

Comparison of Parameters Derived from Dual-Polarization SAR Data and Their Application

Mitsunobu Sugimoto¹, Kazuo Ouchi¹, Yasuhiro Nakamura¹

¹ Department of Computer Science, National Defense Academy

1-10-20 Hashirimizu, Yokosuka, Kanagawa 239-8686 Japan

email: ed10003@nda.ac.jp, ouchi@nda.ac.jp, yas@nda.ac.jp

1. Introduction

The goal of this study is to examine the potential of deriving information comparable to quad-polarization data from dual-polarization data acquired by synthetic aperture radar (SAR). SAR has been proven to be one of the most useful sensors in remote sensing because of its high resolution and all-weather day-and-night observation capabilities. In early days, most SAR systems operated on single-polarization. However, recent technological advancements allowed us to develop and operate SAR systems with multi-polarization observation capability. Multi-polarization data have shown the potential to increase further the ability of extracting physical quantities of observation targets. While quad-polarization data have several advantages, they are relatively few compared with single- or dual-polarization data because of the operational costs and system constraints required for quad-polarization SAR systems. For those reasons, although there are many platforms that can be operated on quad-polarization mode, they are more often to be operated on single- or dual-polarization mode instead. Since there is a certain trade-off between data availability and multi-polarization, we focused on dual-polarization data as a good compromise between single- and quad-polarization data. In this study, we investigated alternative parameter candidates for dual-polarization data. Dual entropy/alpha decomposition and coherence analysis are used in this study. They are one of the methods that can effectively utilize dual-polarization data. Experimental results showed that dual-polarization data can be as capable as quad-polarization data.

2. Alternative parameters

In Pauli decomposition, which is used with quad-polarization data, the data are decomposed into three components: odd-bounce scattering, even-bounce scattering, and volume scattering. Among them, the odd-bounce and even-bounce components can be obtained from HH-VV dual-polarization data. The remaining component, the cross-polarization (closely related to volume scattering) component, cannot be directly obtained from HH-VV dual-polarization data. In place of the cross-polarization component, several parameters derived from HH-VV dual-polarization data can possibly be considered as alternative parameters.

Entropy/alpha decomposition [1] was originally proposed for quad-polarization data, but modified and applied to dual-polarization data later [2] [3]. The entropy/alpha decomposition for dual-polarization data can be expressed as follows:

$$\langle [C_{coh}] \rangle = [U] \begin{bmatrix} \lambda_1 & 0 \\ 0 & \lambda_2 \end{bmatrix} [U]^*{}^T = \lambda_1 \mathbf{u}_1 \mathbf{u}_1^*{}^T + \lambda_2 \mathbf{u}_2 \mathbf{u}_2^*{}^T \quad (1)$$

$$[U] = \begin{bmatrix} U_{11} & U_{12} \\ U_{21} & U_{22} \end{bmatrix} = [\mathbf{u}_1 \quad \mathbf{u}_2] \quad (2)$$

$$\mathbf{u}_i = [\cos \alpha_i \quad \sin \alpha_i e^{j\delta_i}]^T \quad (3)$$

where $\langle[C_{coh}]\rangle$ is averaged coherency matrix, $\lambda_1 \geq \lambda_2$ are eigenvalues, and $[U]$ is orthogonal unitary matrix. $*$ and T denote complex conjugate and transpose respectively. Entropy H and scattering angle $\bar{\alpha}$ and can be expressed as

$$H = -P_1 \log_2 P_1 - P_2 \log_2 P_2 \quad (4)$$

$$\bar{\alpha} = P_1 \cos^{-1}(|U_{11}|) + P_2 \cos^{-1}(|U_{12}|) \quad (5)$$

where

$$P_i = \frac{\lambda_i}{\lambda_1 + \lambda_2} \quad (6)$$

The backscattering of cross-polarization component is relatively large in urban or forested areas and small on the sea. Entropy has a similar trend to cross-polarized scattering. On the other hand, HH-VV coherence is expected to be high on ocean surface or bare soil where surface scattering is dominant and volume scattering is little, and it is low in the areas such as forests where volume scattering is dominant. Thus, HH-VV coherence shows an opposite tendency to the cross-polarization component. In this case, the coherency is modified so that it shows similar trend to the cross-polarized scattering component. The modified coherence between HH and VV polarization is described as follows:

$$\gamma_{coh} = 1 - \frac{|\langle S_{HH} S_{VV}^* \rangle|}{\sqrt{\langle S_{HH} S_{HH}^* \rangle \langle S_{VV} S_{VV}^* \rangle}} \quad (7)$$

where S_{HH} and S_{VV} are complex scattering components of the corresponding polarization combination. In coherence analysis, the phase difference between the two components is also an important factor.

3. Comparison of alternative parameters

We tested possible candidates that can be derived from HH-VV dual-polarization data and can serve as substitutes for cross-polarization component in quad-polarization data. Experiments are performed using the Advanced Land Observation Satellite-Phased Array L-band SAR (ALOS-PALSAR) quad-polarization data. The cross-polarization component is used as a benchmark for alternative parameters. Entropy, scattering angle, modified coherence, and HH-VV phase difference were compared with the cross-polarization component (HV) in quad-polarization data. Fig. 1 shows alternative parameter images of the Tokyo Bay, Japan, compared with the cross-polarization component. The correlation coefficients between the cross-polarization component and alternative parameters are shown in Table 1 with additional results from a different test site (Ishinomaki, Japan).

Table 1: Correlation coefficient between cross-polarization component and alternative parameters.

Parameter	Correlation coefficient	
	Scene 1 (Tokyo Bay)	Scene 2 (Ishinomaki)
Entropy	0.6923	0.6894
Scattering angle	0.7252	0.6363
Modified coherence	0.6854	0.6509
Phase difference	0.7012	0.6620

These values were higher than the correlation coefficient between the components of Pauli decomposition and the corresponding components of four-component decomposition, which were less than 0.6 in those scenes.

4. Extraction of laver cultivation area using alternative parameters

In this section, we will show that the alternative parameters can be applied to practical use. Fig. 2 shows images of Futtu Horn laver cultivation area ($139^\circ 48'E, 35^\circ 17'N$) in Tokyo Bay, Japan. The data were acquired on October 20, 2011 and December 26, 2008 respectively by TerraSAR-X dual-polarization mode (HH and VV). Every year, starting from October, laver cultivation nets are placed at

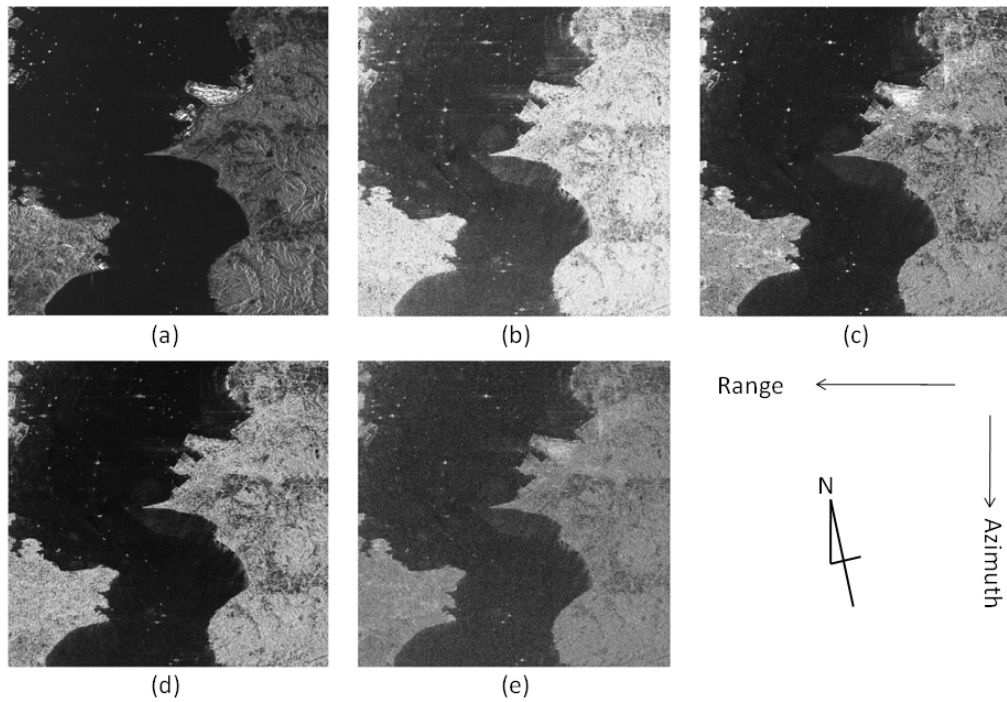


Figure 1: Comparison of alternative parameters. (a) HV (cross-polarized component) (b) entropy (c) scattering angle (d) modified coherence (e) phase difference

approximately 10-20 cm below the sea surface with supporting floats with laver spores attached to the nets, grow during winter, and the grown laver is harvested in April. Through this process, the nets are sometimes placed above the sea surface to promote photosynthesis. When the nets are placed underwater, the areas become effectively shallow water, and small-scale waves, that are the principal scatterers, are damped, resulting in reduced radar backscatter. In Fig. 2 (a) (b), the amplitude of the net areas is higher than background area. Thus, it can be assumed that the nets were above the sea surface. On the other hand, in Fig. 2 (d) (e), the amplitude of net area is lower than the background area and the nets seem to have been placed underwater. Table 2 shows contrast between laver cultivation area and background area. In both data, modified coherence showed highest contrast compared with other parameters. Increased contrast can be seen by comparing the right images (modified coherence image) with the corresponding left and middle images in Fig. 2.

Table 2: Contrast between laver cultivation area and background area in Fig. 2.

Parameter	Contrast	
	2011/10/20	2008/12/26
HH	0.1414	0.2166
VV	0.0529	0.2020
HH+VV	0.0013	0.2122
HH-VV	0.3273	0.2043
Entropy	0.2531	0.4027
Scattering angle	0.3479	0.0065
Modified coherence	0.4790	0.4874
Phase Difference	0.2257	0.0048

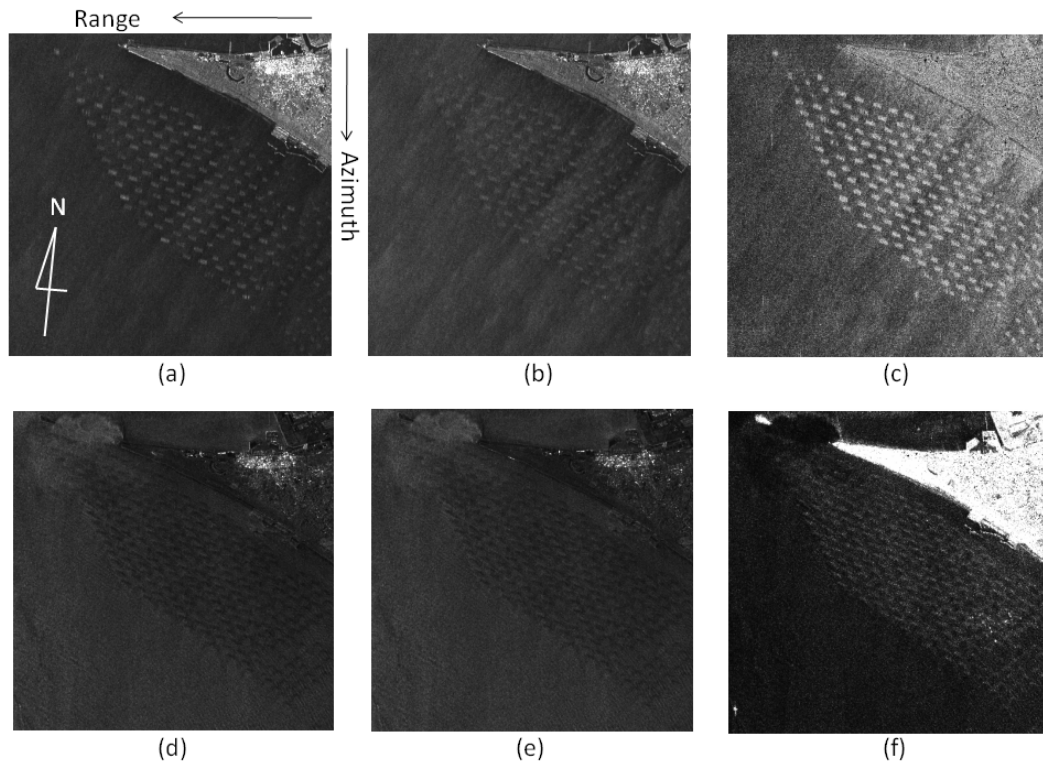


Figure 2: TerraSAR-X images of Futtu Horn laver cultivation area in Tokyo Bay, Japan. The data were acquired on October 20, 2011 (upper row (a), (b), and (c)) and December 26, 2008 (lower row (d), (e), and (f)), respectively. (a)(d): HH polarization image (b)(e): VV polarization image (c)(f): modified coherence image

5. Conclusion

In this study, we compared the parameters that can be derived from dual-polarization data with cross-polarization component and explored how the parameters can be applied for practical use. Through experimental results, we showed that alternative parameters have good correlation with cross-polarization component, and can be used for better extraction of targets than individual polarization channels. Further analysis on individual parameters on specific targets would be an interesting subject. Although dual-polarization data are often considered to be inadequate compared with quad-polarization data, our study showed the potential that dual-polarization data can be as capable as quad-polarization data.

Acknowledgments

Authors would like to thank JAXA for providing ALOS-PALSAR data and PASCO for providing TerraSAR-X data used in this study.

References

- [1] S. R. Cloude and E. Pottier, "An entropy based classification scheme for land applications of polarimetric SAR", *IEEE Trans. Geosci. Remote Sens.*, vol. 35, no. 1, pp. 68-78, 1996.
- [2] S. Cloude, "The dual polarization entropy/alpha decomposition: a pulsar case study", *Proc. POLIn-SAR*, Frascati, Italy, Jan. 2007.
- [3] Z. Shan, C. Wang, H. Zhang and J. Chen, "H- α decomposition and alternative parameters for dual polarization SAR data", *PIERS Proc.*, Suzhou, China, pp. 1386-1390, Sep. 2011.